Editor Decision: Reconsider after major revisions (28 Mar 2015) by Peter Haynes

Comments to the Author:

The reviewers view on the first version of the paper was, for two referees (1 and 3), publish after minor revision and, for the third referee (2), reject. You provided a revised version of the paper responding to the referees' comments and I, bearing in mind the verdicts on the first version of the paper, sent it only to the referee (2) who had recommended reject. That referee has provided further comments and has essentially not moved away from 'reject' recommendation.

Given this disagreement between the referees, and having read the paper carefully myself, my inclination is to go with the majority view and, in due course, accept the paper. However I think that referee 2 made some good points in their original review and not all of them have been answered convincingly. Also from my own reading of the paper I believe that the presentation can be improved significantly.

So I request that you submit a revised version of the paper, plus appropriate replies, that address the following comments of Referee 2 in particular, and also my own comments which follow. I will then consider it again myself (and would hope to accept it for publication).

Dear Peter,

Thank you very much for taking care of our paper yourself! As reviewer 2 and you suggest, we did change our analysis method: we now take the whole simulation period into account and estimate and show the linear "trend" results for the 11-year period 2001-2011.

We have also considerably changed the description of our methodology as well as some of the conclusions. We hope that the paper reads better now and we addressed all your questions and concerns. Please find our detailed comments below.

Issues raised by Referee 2:

1) The choice to look at 10-year trends: I have some sympathy with the view of referee 2 here. It seems that you have chosen, within your simulations from 1960 to 2100, to focus only on trends certain 10-year periods within each simulation (during which changes in particular external drivers are somewhat similar to those over the observed 2002-2012 period). Referee 2 takes the view that this analysis is fragile because of the sensitivity of inferred trends to details of the time series at the beginning and end of the 10-year periods (or correspondingly, sensitivity to the precise choice of the end points of the 10-year period). You have answered this by saying that you have carried out longer integrations — but the fact is that you are still apparently focusing on a small number of 10—year periods. My own take on this

is that, in using information only from a small number of 10-year periods you are discarding a lot of potentially useful information from your simulations. Have you not considered some other approach, such as, in the spirit of Dessler et al (2014), extracting correlation coefficients (between temperatures and the various drivers) over the whole length of the simulation and then considering the implied change of temperature over a particular 10-year period (given changes in the various drivers over that period).

Thank you very much for your comments and suggestions. We have applied the regression over the whole length of our simulations as you suggested, but only mentioned the results without showing any figures in the previous paper version. Now, we estimate contributions of the different factors from the new method, which is easier to understand for authors and more robust. So, we have replaced all related figures using this method.

2) The deduced effect of increasing GHGs or warming SSTs: You claim in your reply that you are unaware of a well-known long-term predicted increase of tropopause temperatures due to increasing GHGs. I am a little surprised at you saying that, but I agree that the story is complicated. For example, the Kim et al (2013) paper makes the statement in the abstract: in the RCP 8.5 scenario, the models predict robust warming both at the 100 hPa and

ZLR [= temperature minimum] levels, but cooling at the 70 hPa level. One of the problems with your paper is that you choose a single measure of TTL temperature which, I think, is the average over tropical box extending from 16km to 20km — so that averages over the warming in the lower part of that height range and the cooling in the upper part of that height range. In the average the cooling dominates slightly — and you make the statement that there is a weak average cooling trend — but you need to explain more carefully how this relates to previous work and how therefore, perhaps, there is no contradiction. (In your reply to referee 2 you show a time series of 'tropopause temperature' — but by what definition?]

Thank you for your comments. We completely agree with you that the GHGs' impact on the TTL temperature is complicated. We have rephrased the description in the text, and explain warming effects in the upper troposphere and cooling effects in the lower stratosphere of GHGs, which are consistent with previous studies (e.g. Kim et. al., 2013).

The tropopause temperature is the lapse rate tropopause, using the standard WMO (World Meteorological Organization) lapse rate criterion (WMO, 1957). However, since we are focusing on temperatures in the TTL, we finally decide to show the regional averaged temperature (20° S-20° N, 100-70 hPa), instead of the tropopause temperature in Fig. S3.

My own comments:

p3 l19: ‘This recent warming of the TTL is different to previous reported temperature evolutions over the last decades’. Is it? Look at Fueglistaler et al (2013) Fig 4, for example — is 2002-2012 really so unique? To me this is simply interesting interdecadal variability.

Thank you for your comment. We completely agree that the recent TTL warming is closely related to the interdecadal/multidecadal variability, which is consistent with our conclusion: the recent TTL warming is mainly due to internal variability. We have removed this sentence, since it was not helpful and confusion.

p3 l23: ‘which might indicate a climate shift’, see comment above, this statement re a ‘climate shift’ seems amateurish and unnecessary. What do you mean by a ‘climate shift’ in any case?

Thank you for the suggestion, we have deleted this sentence here.

p9 2.4: I’m not sure I understand how you calculate this composite trend — e.g. I find it difficult to interpret (5). More detail would be helpful (enough to allow the reader to repeat the calculation for her/himself). More importantly, perhaps, I don’t understand how the differing magnitudes in the change in the driver over different 10-year periods are taken into account. (For example, in Fig 1a the magnitude in the change in the ‘Total solar irradiance’ is different in each of the chosen 10-year periods — how does that get taken account in generating Figure 3?) If the differences in magnitude are ignored then you should say that explicitly and justify.

Sorry for not addressing the methods clear enough. Now, since we have applied a different method, we adapted the description below and hope that the new method description is clearer now.

p10 l14: (also Figure 1) I think that you are saying that in order to calculate solar-cycle associated trends you have picked out 4 10-year periods — and these are indicated in Figure 1a. My comment is that they could be indicated much more clearly (and this applies even more strongly to other panels of Figure 1 where the straight lines corresponding to chosen 10-year periods are almost invisible). I suggest you put in vertical lines at the beginning and end of each 10-year period.

Thank you very much for your suggestions. We have adapted Figure 1 as you suggested due to the new method.

p11 l12: ‘The time periods of increasing QBO amplitude are selected by the same as the procedure as for the tropical SSTs’ — more detail would be welcome.

Thank you for your comments. We have adapted the descriptions.

p12 l16: ‘Please note’ — omit ‘please’

We have done this update.

p12 l18: ‘seed’ > ‘see’

Corrected.

p13 l9: You are deducing the 'contribution of solar variability' from the difference plot in Figure 3c — but is it not important in some way that the vertical structure in that plot is very different to the vertical structure seen in Figure 2, for example?

Thank you for your comment. Yes, the vertical structure is important for understanding the comprehensive impacts of solar variability on temperatures. However, since we are focusing on the TTL region, the impacts in other areas are not the focus of this paper.

p14 l18: 'zero-line just above the tropopause' — actually I'd say that that zero-line is not far from the middle of your 16-20km region.

Thanks for your comment, we have rephrased this sentence.

p16 l25-27: 'This strengthened tropical upwelling cannot continue further up because of the westerly wind anomalies blocking transport into the subtropics and finally diminishing' — I don't see the justification for this statement — is there some dynamical reasoning behind it?

We have added references (e.g. Simpson et. al., 2009; Flannaghan and Fueglistaler, 2013) here regarding dynamical mechanisms and slightly reformulated this sentence.

p17 l16: 'slows down the transition branch of the BDC' — 'transition branch' is a non-standard term — what do you mean?

Thanks for the comments, we have rephrased this sentence.

p19 l16: 'The QBO may influence the TTL temperature by modifying the BDC'. Actually my reading of Kawatani and Hamilton (2013) is that they are suggesting that changes in the BDC cause changes in the QBO. Are you deliberately intending to suggest the opposite and if so, why?

As addressed by previous studies (e.g. Niwano and Shiotani, 2003; Flury et. al., 2013), there are clear evidences of QBO impacts on the BDC. There are also significant differences in the BDC between our Natural and NOQBO simulations, which only differ in their QBO nudging or no nudging.

Dessler, A. E., et al (2014), Variations of stratospheric water vapor over the past three decades, J. Geophys. Res. Atmos., 119, 12,588–12,598, doi:10.1002/2014JD021712.

Flannaghan, T. and Fueglistaler, S.: The importance of the tropical tropopause layer for equatorial Kelvin wave propagation, J. Geophys. Res., 118, 5160–5175, doi:10.1002/jgrd.50418, 2013.

Flury, T., Wu, D. L., and Read, W. G.: Variability in the speed of the Brewer–Dobson circulation as observed by Aura/MLS, Atmos. Chem. Phys., 13, 4563-4575, doi:10.5194/acp-13-4563-2013, 2013.

Fueglistaler, S., et al. (2013), The relation between atmospheric humidity and temperature trends for stratospheric water, J. Geophys. Res. Atmos., 118, 1052–1074, doi:10.1002/jgrd.50157

Niwano, M., Yamazaki, K., and Shiotani, M.: Seasonal and QBO variations of ascent rate in the tropical lower stratosphere as inferred from UARS HALOE trace gas data, J. Geophys. Res., 108, 4794, doi:10.1029/2003JD003871, 2003.

Simpson, I. R., Blackburn, M., and Haigh, J. D.: The role of eddies in driving the tropospheric response to stratospheric heating perturbations, J. Atmos. Sci., 66, 1347–1365, doi:10.1175/2008JAS2758.1, 2009.

WMO, M. (1957), A three-dimensional science, WMO Bull, 6, 134-138.

Manuscript prepared for Atmos. Chem. Phys. Discuss.
with version 2014/07/29 7.12 Copernicus papers of the LaTeX class copernicus.cls.
Date: 22 April 2015

Quantifying contributions to the recent temperature variability in the tropical tropopause layer

W. Wang[1,2], **K. Matthes**[2,3], **and T. Schmidt**[4]

[1]Freie Universität Berlin, Institut für Meteorologie, Berlin, Germany
[2]GEOMAR Helmholtz-Zentrum für Ozeanforschung Kiel, Kiel, Germany
[3]Christian-Albrechts Universität zu Kiel, Kiel, Germany
[4]Helmholtz Zentrum Potsdam, Deutsches GeoForschungsZentrum (GFZ), Potsdam, Germany

Correspondence to: W. Wang (wuke.wang@fu-berlin.de)

Abstract

The recently observed variability in the tropical tropopause layer (TTL), which features an unexpected warming of ~~1.0~~0.9 K over the past decade (2001–2011), is investigated with a number of sensitivity experiments from simulations with NCAR's CESM-WACCM chemistry-climate model. The experiments have been designed to specifically quantify the contributions from natural as well as anthropogenic factors, such as solar variability (Solar), sea surface temperatures (SSTs), the Quasi-Biennial Oscillation (QBO), stratospheric aerosols (Aerosol), greenhouse gases (GHGs), as well as the dependence on the vertical resolution in the model. The results show that, in the TTL from 2001 through 2011: a cooling in tropical SSTs leads to a weakening of tropical upwelling around the tropical tropopause and hence relative downwelling and adiabatic warming of ~~0.4~~0.3 K decade^{-1}; ~~an increased QBO amplitude results~~ stronger QBO westerlies result in a ~~0.5~~0.2 K decade^{-1} warming; increasing aerosols in the lower stratosphere lead to a ~~0.4~~0.2 K decade^{-1} warming; a prolonged solar minimum ~~and increased GHGs contribute about 0.3 and 0.1~~contributes about 0.2 K decade^{-1} to a cooling~~, respectively.~~ ; and increased GHGs have no significant influence. Considering all the factors mentioned above, we compute a net 0.5 K decade^{-1} warming, which is less than the observed 0.9 K decade^{-1} warming over the past decade in the TTL. Two simulations with different vertical resolution show that~~the vertical resolution can strongly influence the response of the TTL temperature to changes such as SSTs. With~~ , with higher vertical resolution, an extra 0.8 K decade^{-1} warming can be simulated through the last decade, compared with results from the "standard" low vertical resolution simulation. ~~Considering all the factors mentioned above, we compute a net 1.7warming, which is in good agreement with the observed 1.0warming over the past decade in the TTL. The model results indicate that the recent warming in the TTL is mainly due to internal variability, i.e. the QBO and tropical SSTs.~~ Model results indicate that the recent warming in the TTL is partly caused by stratospheric aerosols and mainly due to internal variability, i.e. the QBO and tropical SSTs. The vertical resolution can also strongly influence the TTL temperature response in addition to variability in the QBO and SSTs.

1 Introduction

The TTL is the transition layer from the upper troposphere to the lower stratosphere in the tropics, within which the air has distinct properties of both the troposphere and the stratosphere. The vertical range of the TTL depends on how it is defined, i.e., it can be a shallower layer between 14–18.5 km (Fueglistaler et al., 2009) or a deeper layer of about 12–19 km (Gettelman and Forster, 2002; SPARC-CCMVal, 2010, chapter 7). As a key region for the stratosphere-troposphere coupling, the TTL acts like a "gate" for air entering into the stratosphere from the tropical troposphere. The temperature in the TTL is determined by the combined influences of latent heat release, thermally as well as dynamically driven vertical motion, and radiative cooling (Gettelman and Forster, 2002; Fueglistaler et al., 2009; Grise and Thompson, 2013). The thermal structure, static stability and zonal winds in the TTL affect the two-way interaction between the troposphere and the stratosphere (Flury et al., 2013; Simpson et al., 2009) as well as the surface climate, since the relative minimum temperature (usually known as the cold point tropopause, CPT) subsequently influences the radiation and water vapor budget (Andrews, 2010). The TTL reacts particularly sensitively to anthropogenically induced radiative, chemical and dynamical forcings of the climate system, and hence is a useful indicator for climate change (Fueglistaler et al., 2009).

Over the past decade, a remarkable warming has been captured by Global Positioning System Radio Occultation (GPS-RO) data in the TTL region (Schmidt et al., 2010; Wang et al., 2013). This might indicate a climate change signal, with possible important impacts on stratospheric climate, e.g., ~~the tropical tropopause temperature dominates the~~ tropical tropopause temperatures dominate the amount of water vapor entering the stratosphere ~~.~~(Dessler et al., 2013, 2014; Solomon et al., 2010; Gettelman et al., 2009; Randel and Jensen, 2013). So far a long-term cooling in the lower stratosphere has been reported from the 1970s to 2000, although there are large differences between different data sets (Randel et al., 2009; Wang et al., 2012; Fueglistaler et al., 2013). The exact reason of the recent warming is therefore of great interest. An interesting question is also whether

this warming will continue or change in sign in the future, and how well climate models can reproduce such a strong warming over one decade or longer time periods.

Based on model simulations, Wang et al. (2013) suggested that the warming around the tropical tropopause could be a result of a weaker tropical upwelling, which implies a weakening of the Brewer–Dobson circulation (BDC). However, the strengthening or weakening of the BDC is still under debate (Butchart, 2014, and references therein). Results from observations indicate that the BDC may have slightly decelerated (Engel et al., 2009; Stiller et al., 2012), while estimates from a number of Chemistry-Climate Models (CCMs) show in contrast a strengthening of the BDC (Butchart et al., 2010; Li et al., 2008; Butchart, 2014). The reason ~~of~~ for the discrepancy between observed and modeled BDC changes, as well as the ~~mechanism~~ mechanisms of the BDC ~~in~~ response to climate change, ~~is~~ are still under discussion (Oberländer et al., 2013; Shepherd and McLandress, 2011). The trends in the BDC may be different in different branches of the BDC (Lin and Fu, 2013; Oberländer et al., 2013). Bunzel and Schmidt (2013) show that the model configuration, i.e. the vertical resolution and the vertical extent of the model, can also impact trends in the BDC.

There are a number of other natural and anthropogenic factors besides the BDC, which influence ~~the~~ radiative, chemical and dynamical processes in the TTL. One prominent candidate for natural variability is the sun, which provides the energy source ~~for~~ of the climate system. The 11 year solar cycle is the most prominent natural variation on the decadal time scale (Gray et al., 2010). Solar variability influences the temperature through direct radiative effects and indirectly through radiative effects on ozone as well as indirect dynamical effects. The maximum response in temperature occurs in the equatorial upper stratosphere during solar maximum conditions, and a distinct secondary temperature maximum can be found in the equatorial lower stratosphere around 100 hPa (SPARC-CCMVal, 2010; Gray et al., 2010).

SSTs also influence the TTL by affecting the dynamical conditions and subsequently the propagation of ~~planetary~~ atmospheric waves and hence the circulation. Increasing tropical SSTs can enhance the BDC, which in turn cools the tropical lower stratosphere through enhanced upwelling (Grise and Thompson, 2012, 2013; Oberländer et al., 2013). The QBO is

the dominant mode of variability throughout the equatorial stratosphere, and has important impacts on the temperature structure as well as the distribution of chemical constituents like water vapor, methane and ozone (Baldwin et al., 2001). ~~which is maximized~~ Stratospheric aerosols absorb outgoing long-wave radiation and lead to additional heating in the lower stratosphere, which maximizes around 20 km (Solomon et al., 2011; SPARC-CCMVal, 2010, chapter 8).

While GHGs warm the troposphere, they cool the stratosphere at the same time by releasing more radiation into space. Warming of the troposphere and cooling of the stratosphere affect the temperature in the TTL directly, and also indirectly, by changing chemical trace gas distributions and wave activities (SPARC-CCMVal, 2010).

In climate models, a sufficient high vertical resolution is important in order for models to correctly represent dynamical ~~process~~processes, such as wave propagation into the stratosphere and wave-mean flow interactions. ~~It is a prominent factor for a climate model~~ High-vertical resolution is also important to generate a self-consistent QBO (Richter et al., 2014). Meanwhile, vertical resolution is essential for a proper representation of the thermal structure in the model, e.g. models with coarse vertical resolution can not simulate the tropopause inversion layer (TIL, a narrow band of temperature inversion above the tropopause associated with a region of enhanced static stability) well (Wang et al., 2013; SPARC-CCMVal, 2010, chapter 7). Coarse vertical resolution is also still a problem for analysing the effects of El-Niño Southern Oscillation (ENSO) and the QBO onto the tropical tropopause (Zhou et al., 2001; SPARC-CCMVal, 2010, chapter 7).

In this study we use a series of simulations with NCAR's Community Earth System Model (CESM) model (Marsh et al., 2013), to quantify the contributions of the above discussed factors – Solar, SSTs, QBO, Aerosol and GHGs – to the recently observed variability in the TTL.

The details of the ~~observed~~ observational data, the model and numerical experiments, as well as a description of our methods are given in Sect. 2. The observed temperature variability in the TTL and the contributions of various factors to the recent TTL variability are

addressed in Sect. 3. Section 4 focuses on the importance of the vertical resolution in one climate model. A summary and discussion are presented in Sect. 5.

2 Model simulations and method description

2.1 Fully-coupled CESM-WACCM simulations

The model used here is NCAR's Community Earth System Model (CESM), version 1.0. CESM is a fully coupled model system, including an interactive ocean (POP2), land (CLM4), sea ice (CICE) and atmosphere (CAM/WACCM) component (Marsh et al., 2013). As the atmospheric component we use the Whole Atmosphere Community Climate Model (WACCM), version 4. WACCM4 is a chemistry–climate model (CCM), with detailed middle atmospheric chemistry and a finite volume dynamical core, extending from the surface to about 140 km (Marsh et al., 2013). The standard version has 66 (W_L66) vertical levels, which means about 1 km vertical resolution in the TTL and in the lower stratosphere. All simulations use a horizontal resolution of $1.9^\circ \times 2.5^\circ$ (latitude $\times$ longitude) for the atmosphere and approximately 1 degree for the ocean.

Table 1 gives an overview of all coupled CESM simulations. A control run was performed from 1955 to 2099 (Natural run hereafter), with all natural ~~forcings~~ forcing including spectrally resolved solar variability (Lean et al., 2005), a fully coupled ocean, volcanic aerosols following the SPARC ~~CCMVal~~ (Stratospheric Processes and their Role in Climate) CCMVal (Chemistry-Climate Model Validation) REF-B2 scenario recommendations (see details in SPARC-CCMVal, 2010) and a nudged QBO. The QBO is nudged by relaxing the modeled tropical zonal winds to observations between 22° S and N, using a Gaussian weighting function with a half width of 10° decaying latitudinally from the equator. Full vertical relaxation extends from 86 to 4 hPa, which is half the strength of the level below and above this range and zero for all other levels (see details in Matthes et al., 2010; Hansen et al., 2013). The QBO forcing time series in CESM is determined from the observed climatology of 1953-2004 via filtered spectral decomposition of that climatology. This gives a set of

Fourier coefficients that can be expanded for any day and year in the past and the future. Anthropogenic forcings like GHGs and ozone depleting substances (ODSs) are set to constant 1960s conditions. Using the Natural run as a reference, a series of four sensitivity experiments were performed by systematically switching on or off several factors. The SolarMean run uses constant solar cycle values averaged over the past 4 observed solar cycles; the FixedSST run uses monthly varying climatological SSTs calculated from the Natural run, and therefore neglects variability from varying SSTs such as ENSO; in the NOQBO run the QBO nudging has been switched off which means weak zonal mean easterly winds develop in the tropical stratosphere. An additional simulation RCP85, uses the same forcings as the Natural run, but in addition includes increases in anthropogenic GHGs and ODSs forcings. These forcings are based on observations from 1955 to 2005, after which they follow the Representative Concentration Pathways (RCPs) RCP8.5 scenario (Meinshausen et al., 2011).

2.2 WACCM atmospheric stand-alone simulations

Instead of using the fully coupled CESM-WACCM version, WACCM can be integrated in an atmospheric stand-alone configuration, with prescribed SSTs and sea ice. Beside the standard version with 66 vertical levels (W_L66), we have also performed simulations with a finer vertical resolution, with 103 vertical levels and about 300 m vertical resolution in the TTL and lower stratosphere (W_L103) (Gettelman and Birner, 2007; Wang et al., 2013).

With the ~~stand-alone atmospheric version~~ atmospheric stand-alone version, an ensemble of three experiments was performed over the recent decade 2001–2010 with both WACCM versions (W_L66, W_L103) (see Table 2). Observed SSTs and spectrally resolved solar fluxes were used to produce the most realistic simulations of atmospheric variability over the past decade (2001–2010). The QBO is nudged using the same method as in the fully-coupled runs discussed above. GHGs and ODSs are based on observations for the first 5 years (2001–2005) and then follow the IPCC RCP4.5 scenario for the next 5 years (2005–2010), since no ~~observed~~ observational data were available when the simulations were started. Atmospheric aerosols were relatively constant between 2001 and 2010 since no

strong volcanic eruptions occurred, and are the same as in the CESM-WACCM runs described above. All the forcings considered in this study are available from the CESM model input data repository (https://svn-ccsm-inputdata.cgd.ucar.edu/trunk/inputdata/). An additional run (W_Aerosol) was performed using the W_L103 version with observed, more realistic stratospheric aerosol ~~forcings~~ forcing from the Chemistry-Climate Model Initiative (CCMI, http://www.met.reading.ac.uk/ccmi/)~~project~~.

2.3 ~~Linear trend calculation~~Estimation of factor contributions

~~A standard least square regression is used to calculate the linear trend. For example, using time (t) as a single predictor, the predicted temperature (T) can be expressed as: where the subscript "est" indicates that this is an estimate of T, and "b" represents the linear trend. The residuals are defined by the differences between the actual and the estimated temperature The "best-fit" is defined by the line that minimizes the sum of the squares of the residuals. The seasonal cycle was removed from the temperature time series before doing the regression.~~ For a pair of reference and single-factor runs (e.g. Natural and SolarMean), all configuration and drivers are the same except for the long-term variability of the respective factor (e.g. Solar). Temperature differences $T_{\text{diff}}(x,t)$ between the reference and single-factor runs (e.g. Natural - SolarMean) can be estimated by a linear regression:

$$T_{\text{est}}(x,t) = c(x)X(t), \tag{1}$$

where $T_{\text{est}}(x,t)$ is an estimate of $T_{\text{diff}}(x,t)$ at each grid point (x) and each simulation time (t). $X(t)$ is the time series of the respective factor (e.g. Solar) and $c(x)$ are the coefficients of that factor at each grid point.

Then the contributions of that factor to the recent warming in the TTL can be estimated as:

$$T_{\text{fac}}(x) = c(x)b_{\text{fac}}, \tag{2}$$

where $T_{\text{fac}}(x)$ represents the factor contribution to the recent temperature trend, $c(x)$ are the coefficients and b_{fac} is the observed linear trend of that factor during 2001-2011 (Fig. 1).

The standard error (SE) ~~is~~ can be used to estimate the uncertainty of the ~~estimated trend~~regressed coefficients $c(x)$, which is defined by:

$$(\text{SE})^2 = \left[\sum_{t=1}^{n} e_t^2\right] / \left[(n_{\text{eff}} - 2)\sum_{t=1}^{n}(X_t - \bar{X})^2\right], \tag{3}$$

where n is the sample size, ~~and t~~ $e = T_{\text{diff}} - T_{\text{est}}$ are the residuals, and $\bar{X}$ is the mean value. ~~The smaller this standard error is , the more certain is the trend.~~

~~If the trend is larger than two times the standard error, the linear regression is statistically significant at the 95confidence level. A brief description of the least square regression, the uncertainty of the trend, as well as the significance testing can be found in~~ n_{eff} is the effective number of degrees of freedom, with consideration of the effect of autocorrelation, which is determined by:

$$n_{\text{eff}} = n\frac{1 - r_{\text{a}}}{1 + r_{\text{a}}}, \tag{4}$$

where r_{a} is the lag-1 autocorrelation coefficient (Wigley, 2006).

2.4 ~~Composite method~~

For the estimated coefficients c, the test statistics

$$t\_test = \frac{c}{SE}, \tag{5}$$

has the Student's t-distribution with $n_{\text{eff}} - 2$ degrees of freedom.

~~To estimate the contribution of the different factors to the observed temperature variability in the TTL, the composite for each factor is computed following three steps: (1) calculation~~

~~of the linear trend for the respective factor over the past decade (2001–2011) from the observed, deseasonalized time series, (2) selection of time periods in the reference run, which are similar to the observed trends for the respective factor (the method of selection and the number of similar time periods depends on the factor, see below), and (3)~~ Beside the regressions described above, the Pearson's correlations (r) between temperature differences (T_{diff}) and the respective factor (X) were also estimated. The test statistics

$$t\_test = r\sqrt{\frac{n_{\text{eff}} - 2}{1 - r^2}}, \tag{6}$$

has the Student's t-distribution with $n_{\text{eff}} - 2$ degrees of freedom, and the effective number of degrees of freedom can be estimated by:

$$\frac{1}{n_{\text{eff}}} = \frac{1}{n} + \frac{2}{n} r_{\text{a1}} r_{\text{a2}}, \tag{7}$$

where r_{a1}, r_{a2} are the lag-1 autocorrelation coefficients of the two time series in calculating the Pearson's correlation, respectively.

Such regressions, correlations and 11-year trend estimations were applied to all factors, i.e., Solar, SSTs, QBO, GHGs and stratospheric aerosols.

Special attention is given to the region 20° S–20° N latitude and 16–21 km height, which is mainly the observed warming area in the TTL (see below). Hereafter, we use the average trend over this area to discuss the exact contribution of every factor to the temperature trend in the TTL.

2.4 Forcings in observations and model simulations

~~Figure 1 shows the time series of both natural and anthropogenic forcings over past and future decades in the observations (black) and in the Natural model experiment (blue). Periods with a similar trend as the recent decade (2001–2011) are shown with straight~~

lines. Figure 1 shows the time series of both natural and anthropogenic forcings over past and future decades in observations (black) and model experiments (blue). Observed linear trends during 2001–2011 are highlighted with straight lines.

Observations of the solar variability show that the total solar irradiance (TSI) exhibits a clear 11 year solar cycle (SC) variation of about 1 W m^{-2} between sunspot minimum (S_{min}) and sunspot maximum (S_{max}) in the past (Gray et al., 2010), with a delayed and smaller amplitude return to maximum conditions in the recent decade (Fig. 1a). . The future projection in the Natural run is a repetition of the last four observed solar cycles (Fig. 1a, blue line). With a delayed and smaller amplitude return to maximum conditions, the observed TSI significantly (over 95 %) decreased during 2001-2011 (Fig. 1a, straight black line). Similar periods of decreasing TSI can be found in the periods 1958–1968, 2001–2011, 2045–2055, and 2089–2099. A composite trend is then constructed by applying multiple linear regression to all four selected periods in the Naturalas well as the SolarMeanexperiments (Eq. 5) . By comparing the trends in these two runs with and without solar cycle variations, the effect of solar variability on the temperature trend in the TTL can be estimated.

Figure 1b shows the variability of tropical (20° S–20° N) SSTs for the last five decades from observations (Hadley Center Updates and supplementary information available from http://www.metoffice.gov.uk/hadobs/hadisst, black lines) and up to 2099 from the Natural coupled CESM-WACCM model experiment (blue line). Both the observed and simulated tropical SSTs show a statistically significant (over 95 %) decrease from 2001 to 2011. A similar decrease in tropical SSTs can be found during the periods 1956–1968, 1980–1991, 2001–2014, 2028–2043 and 2047–2057. Periods longer than 10years have been selected from the filtered tropical SST time series. Filtering has been performed twice with a Butterworth low-pass filter (longer than 30years). Note that there is also a strong drop in SSTs around 1992 in the model, which does not occur in the observations. This might be caused by an overestimated response to the Pinatubo eruption in the CESM-WACCM model (Marsh et al., 2013; Meehl et al., 2012). By comparing the Natural run, where SSTs

~~are calculated explicitly, and the FixedSST run where SSTs are climatologically prescribed, the effect of interactively calculated SSTs can be determined.~~

~~Instead of a decrease in tropical SSTs, the QBO amplitude shows an increase during the selected two periods (Fig. 1c). The observed QBO amplitude has been calculated from the absolute values of deseasonalized monthly mean anomalies of the zonal mean zonal wind at 70(from the FU Berlin:); in our model simulations it is computed where the QBO has been nudged. The time periods of increasing QBO amplitude are selected by the same as the procedure as for the tropical SSTs. By comparing the Natural and the NOQBO experiments, the effect of a (nudged) QBO on the temperature trends in the TTL can be estimated.~~ The QBO variations are represented by a pair of orthogonal time series QBO1 and QBO2, which are constructed from the equatorial zonal winds over 70-10 hPa (Randel et al., 2009). The observed QBO2 (data from the FU Berlin: http://www.geo.fu-berlin.de/en/met/ag/strat/produkte/qbo/index.html), which is the dominate mode of QBO in the tropical lower stratosphere, shows an increase (towards westerlies shift) during 2001-2011 (Fig. 1c, straight black line). Note that this linear trend of the QBO2, especially during a short period, is very sensitive to the start and ending years depending on the QBO phase (a further analysis for 2001-2012, ending with a relative minimum of QBO2, indicates a weaker but still significant increase).

As shown in Fig. 1d, GHGs show a steady increase after 2001. The increasing rate of global CO_2 release from 2001 to 2011 is close to the RCP8.5 scenario, which ~~we~~ were used in our RCP85 run. ~~By comparing the experiments with (RCP85) and without (Natural) GHG increases, the GHG effect on the observed temperature trend can be estimated.~~

Similar to the GHGs, observed stratospheric aerosols (aerosol optical depth (AOD)) have been steadily increasing since 2001 (Solomon et al., 2011) in the lower stratosphere (18–32 km) (Fig. 1e). This increase in stratospheric aerosol loading is attributed to a number of small volcanic eruptions and anthropogenically released aerosols transported into the stratosphere during the Asian Monsoon (Bourassa et al., 2012; Neely et al., 2013). An aerosol data set has been constructed for the CCMI project (ftp://iacftp.ethz.ch/pub_read/luo/ccmi/) and is similar to the data described by

Solomon et al. (2011). The comparison of the two experiments with different AOD data sets will shed light on the stratospheric aerosol contribution to the observed temperature trend.

All natural and anthropogenic forcings will be discussed with respect to their contribution to the temperature variability in TTL in the following section.

3 Quantification of observed temperature variability

3.1 Observed temperature variability in the TTL

Figure 2 shows the latitude-height section of the linear temperature ~~trend~~ trends for the period 2001–2011 estimated from GPS-RO observations (see details of the GPS-RO data in Wang et al. (2013)). A remarkable and statistically significant warming occurs around the TTL between about 20° south to north and from ~~15 to 20~~16 to 21 km height. The warming in the TTL is ~~1.0~~ 0.9 K decade^{-1} on average, with a maximum of about 1.8 K decade^{-1} directly at the tropical tropopause around 17 to 18 km. This figure is an extension of earlier work by Schmidt et al. (2010) and Wang et al. (2013) and shows an unexpected warming, despite the steady increase in GHGs~~which imply a cooling of this region~~. Therefore it is interesting to study whether this warming is simply a phenomenon of the past decade and the result of internal atmospheric variability, or whether it will persist for longer and therefore modify trace gas transport from the troposphere into the stratosphere.

Note that this decadal warming in the TTL may vary in magnitude if different end years are selected due to the relative short length of the time series. The warming is weaker if end years of 2012 or 2013 are chosen (see also Figs. S1 and S2). In the following investigations, we keep the period from 2001 through 2011 to be most consistent with our stand-alone WACCM simulations (2001–2010). We will explain the temperature variability within a time period of about one decade. This decadal variability may change sign from decade to decade if it is mainly caused by natural/internal variability. However, it is still very important to understand the reasons and mechanisms behind these internal variability modes as it might eventually enhance our decadal to multi-decadal predictive skills.

3.2 Contribution of solar variability

Figures 3a and b show the ~~composite temperature trends for periods with decreasing solar irradiance (1958–1968, 2001–2011, 2045–2055, and 2089–2099) for the Natural and SolarMeanruns, respectively. The Natural run shows a partially significant temperature increase from S_{max} to S_{min} of about~~ correlation between temperature differences (Natural - SolarMean) with solar forcing (TSI) in the Natural run over the whole simulation period from 1955 through 2099, as well as the estimated temperature trends during 2001 through 2011 related to a decreasing total solar irradiance (TSI). The correlation between temperature differences and TSI is relatively weak, amounts to less than 0.1 ~~on average around the TTL , while the SolarMean run shows on average a partially statistically significant temperature increase of 0.4in the tropics and subtropics. Figure 3c shows the differences in temperature trends between the Natural and the SolarMean experiments. Solar variability thus~~ in the TTL region and is a little higher and more significant in the lower stratosphere. With such a weak positive correlation, the decreasing solar irradiance contributed to a cooling of about ~~0.3–0.2~~ K decade^{-1} in the TTL during ~~periods with similar solar variability to the recent decade~~2001–2011.

3.3 Contribution of tropical SSTs

Figure 4 shows the ~~composite temperature trends for the periods with decreasing tropical SSTs (1956–1968~~correlation between temperature differences (Natural - FixedSST) with tropical (20°S-20°N) SSTs from the Natural run over the whole simulation period from 1955 through 2099, ~~1980–1991, 2001–2014, 2028–2043 and 2047–2057) for both the Natural and the FixedSST runs (Fig. 4a and b),~~ as well as ~~their differences (Fig. 4c) . While the Natural experiment shows a partially statistically significant temperature increase of 0.4on average (1.0in maximum) in the TTL, the FixedSST experiment shows an insignificant (0–0.2) temperaturechange during periods with similar SST variability to the recent decade~~the estimated temperature trends from 2001 through 2011 due to decreasing tropical SSTs. Temperature differences are closely correlated with tropical SSTs, which

show strong positive correlations (up to 0.8) below and significant negative correlations (over 0.5) above the tropopause in the tropics. The strong correlation between tropical SSTs and atmospheric temperatures indicates that tropical SSTs have important impacts on the TTL temperature. A decrease in tropical SSTs contributes therefore to a statistically significant warming of ~~0.4~~ 0.3 K decade^{-1} on average (0.6 K decade^{-1} in maximum) in the TTL during 2001–2011 (Fig. 4c).

3.4 Contribution of the QBO

~~Figures 5a and b show composite temperature trends, for periods with increasing QBO amplitudes (2003–2017 and 2054–2068) for the~~ As described in *section*2.5, a pair of orthogonal time series of the QBO are used in the regression between temperature differences (Natural ~~-~~ NOQBO) and the ~~NOQBO experiment, respectively. While the Natural experiment shows an insignificant warming of 0.3on average (0.8in maximum)~~ QBO from the Natural run. Since the QBO1 mainly affects temperature at middle and upper stratosphere, only the QBO2 correlation and impacts are shown in Figure 5. QBO2 features a strong positive correlation in the TTL ~~, the NOQBO run shows a slight but statistically significant cooling for the same period. The differences in Fig. 5c indicate that the increased QBO amplitude~~ region, which amounts up to 0.6. An observed increase of QBO2 during 2001–2011 therefore contributes to a ~~warming of 0.5~~ 0.2 K decade^{-1} warming on average (~~0.8~~0.4 K decade^{-1} in maximum) in the TTL. Another effect of the QBO is the statistically significant cooling trend seen in the tropical middle stratosphere above ~~22~~23 km~~in the Natural run~~. This QBO effect may help to explain the observed tropical cooling (see Fig. 2). ~~Please note, however, that,~~ However, CESM1.0 used for these simulations, cannot generate a self-consistent QBO and hence uses wind nudging, which might cause problems when estimating QBO effects on temperature variability in the tropical lower stratosphere (Marsh et al., 2013; Morgenstern et al., 2010).

3.5 Contribution of GHGs

The temperature trends from both the Natural and the RCP85 experiments between 2001 and 2050 are shown in Figs. 6a and b, respectively. As expected, increasing As expected, GHGs show strong positive correlations with temperatures in the troposphere and significant negative correlations with temperatures in the stratosphere, with a switch of sign near the tropopause (about 18 km). Increasing GHGs in the RCP85 experiment tend to cool the lower stratosphere and warm the upper troposphere, with a zero line slightly above the tropopause . Hence the effect of global warming is seen in Fig. 6c with a weak averaged cooling trend in the TTL of about 0.1 . but have no evident contribution around the tropopause (with a change of correlation sign at about 18 km). This is consistence with previous studies (e.g. Kim et al., 2013), which confirmed a warming at 100 hPa (below the tropopause) and a cooling at 70 hPa (above the tropopause) due to the increase of GHGs in CMIP5 (Coupled Model Intercomparison Project Phase 5) simulations.

3.6 Contribution of stratospheric aerosols

The temperature trends from the simulations with relative constant AOD values correlations between temperature differences (W SUBSCRIPTNBLA103) and with more realistic CCMI aerosols (erosol - W SUBSCRIPTNBALerosol) 103) with CCMI stratospheric aerosols, as well as the contributions of increasing stratospheric aerosols to the recent warming in the TTL are shown in Figs. 7a and b, respectively. A clearly stronger and more statistically significant warming pattern can be seen around the tropical tropopause in the WSUBSCRIPTNBAerosol run as compared to the WSUBSCRIPTNBL103 runWeak but partly significant correlations of stratospheric aerosols to temperature in the TTL can be found in Fig. 7a, with a change of correlation sign below the tropopause (about 15 km) and up to 0.2 in the lower stratosphere. The effect of increasing stratospheric aerosols during 2001–2011 is estimated to be 0.4 0.2 K decade^{-1} warming in the TTL (Fig. 7c). 7b). Note that there may exist uncertainties for this result since we have only 10 years of simulations

for the W
SUBSCRIPTNBAerosol run.

4 Effects of the vertical resolution

To estimate not only anthropogenic and natural contributions to the recent TTL temperature variability but also the effects of the vertical resolution in the model, Figs. 8a and b show the temperature trends in the standard W_L66 run and the differences in temperature trends between the high-resolution (W_L103) and the standard (W_L66) runs, respectively. The W_L103 run (Fig. 8b) shows a statistically significant ~~0.6~~0.5 K decade^{-1} warming on average over the past decade around the TTL, which maximizes at 1.2 K decade^{-1}. The standard W_L66 run (Fig. 8a) does not capture the warming. The only difference between the two experiments is the vertical resolution, meaning that a higher vertical resolution captures the warming in the TTL better than the standard vertical resolution, reaching up to 0.8 K decade^{-1} (Fig. 8b). Wang et al. (2013) showed that the tropical upwelling in the lower stratosphere has weakened over the past decade in the W_L103 run, while there is no significant upwelling trend in the standard vertical resolution (W_L66) run. The decreasing tropical upwelling in the W_L103 run might be the reason for the extra warming in the TTL compared to the W_L66 run, since dynamical changes would lead to adiabatic warming. More detailed ~~investigation~~ investigations will be given in the following section.

4.1 Changes in the Brewer–Dobson circulation

To investigate dynamical differences between the two experiments with standard and higher vertical resolution in more detail, the Transformed Eulerian Mean (TEM) diagnostics (Andrews et al., 1987) was applied to investigate differences in the wave propagation and Brewer–Dobson circulation (BDC) in the climatological mean as well as in the decadal trend.

Figure 9 shows the annual mean climatology of the BDC (arrows for the meridional and vertical wind components), the zonal mean zonal wind (blue contour lines) and the tem-

perature (filled colours) from the W_L103 run (Fig. 9a), as well as the differences between the W_L103 and the W_L66 runs (Fig. 9c). The BDC shows an upwelling in the tropics and a downwelling through mid to high latitudes in the annual mean. With finer vertical resolution (W_L103) the model produces a stronger upwelling in the tropics (and a consistent cooling) up to the tropopause region, with westerly wind anomalies above. This strengthened tropical upwelling cannot continue further up because of the westerly wind anomalies which block the transport into the subtropics (Simpson et al., 2009; Flannaghan and Fueglistaler, 2013). Above the tropical tropopause there is less upwelling and in particular more transport from the subtropics into the tropical TTL, leading to a stronger warming around 19 km in the W_L103 experiment. These changes in the BDC indicate a strengthening of its lower branch, and a weakening ~~of the~~ at upper levels in the lower stratosphere (Lin and Fu, 2013). This is consistent with previous work by Bunzel and Schmidt (2013), which indicates a weaker upward mass flux around 70 hPa in a model experiment with higher vertical resolution.

The annual mean trends in the W_L103 experiment indicate a further strengthening of the BDC lower branch over the past decade in this simulation (Fig. 9b) and a statistically significant weakening ~~of the~~ in the lower stratosphere resulting in significant warming of 1 to 2 K decade^{-1} in the TTL. In particular the trends in the TTL are stronger in the W_L103 compared to the W_L66 experiment (Fig. 9d). ~~This is consistent with previous work by , which shows also stronger changes in the BDC using a model with higher vertical resolution.~~

In summary, the finer vertical resolution can enhance the upward wave propagation from the tropics. This enhanced wave propagation speeds up the lower branch of the BDC in the upper troposphere and slows down ~~the transition branch of the BDC~~the upper branch of the BDC in the lower stratosphere. These changes in the BDC and corresponding wave-mean flow interactions (not shown) finally result in the statistically significant warming in the TTL.

Bunzel and Schmidt (2013) attributed the differences in the BDC to different vertical resolutions which tend to reduce the numerical diffusion through the tropopause and the secondary meridional circulation. Our results show that the strong warming and subsequent

enhanced static stability (not shown) above the tropopause may also influence wave dissipation and propagation around the tropopause. Oberländer et al. (2013) point out that an increase of tropical SSTs enhances the BDC. This is consistent with our results, which show a weakening of the BDC in the lower stratosphere following a decrease in tropical SSTs. At the same time, this response of the stratosphere to the surface can be better represented by a model with finer vertical resolution.

5 Summary and discussion

Based on a series of sensitivity simulations with NCAR's CESM-WACCM model, the relationships between different natural (solar, QBO, tropical SSTs) and anthropogenic (GHGs, ODS) factors and temperatures around TTL, as well as their contributions to the observed warming of the TTL over the past decade from 2001 through 2011 has been studied. By regressing the temperature differences between model experiments to the respective factors for the whole simulation periods between 1955 through 2099, and projecting the regressed coefficients onto the observed trends of the respective factor during 2001-2011, the contribution of ~~different natural (solar, QBO, tropical SSTs) and anthropogenic (GHGs, ODS) factors to the observed warming of the TTL over the past decade from 2001 through 2011 has been studied. By comparing model experiments with and without the respective factors and combining a number of periods with similar trends in a composite, the contribution of~~ each factor has been quantified in order to explain the causes of the observed recent decadal variability seen in GPS-RO data.

The SSTs show strong significant negative correlation (-0.5) with temperatures in the TTL, while the QBO2 shows a reversed pattern (0.6). The TSI and stratospheric aerosols result in weak positive correlations (0.1-0.2) with TTL temperatures. GHGs show positive correlations with temperatures in the troposphere and negative correlations with temperatures in the stratosphere, while there is no significant correlation around the tropopause.

A decrease in tropical SSTs, an increase in stratospheric aerosol loading and ~~an increase in the QBO amplitude~~ stronger QBO westerlies contribute each about ~~0.4, 0.4 and 0.5~~0.3, 0.2 and 0.2 K decade^{-1} to this warming, respectively, resulting in a total ~~1.3~~0.7 K decade^{-1} warming, while the delay and smaller amplitude of the current solar maximum ~~and the steady increase in GHGs and ODS concentrations contribute each about 0.3 and 0.1~~contributes about 0.2 K decade^{-1} to a cooling~~, respectively, resulting in a total 0.4cooling. The vertical resolution of the model strongly influences the TTL response to the surface mainly via dynamical changes, i.e. an enhancement of the lower branch of the BDC and a decrease of the transition (upper) branch in response to the decreasing tropical SSTs.~~ . Adding all natural and anthropogenic factors, we estimate a total modeled warming of 0.5 K decade^{-1} around the TTL (Table 3), which is less than the observed 0.9 K decade^{-1} warming from GPS-RO data. One possible reason of this weak estimate is the relative low vertical resolution of the model, which strongly influences the TTL response to the surface mainly via dynamical changes, i.e. an enhancement of the lower branch of the BDC and a decrease of the upper branch in the lower stratosphere in response to decreasing tropical SSTs. This leads to a 0.8 K decade^{-1} extra warming in the TTL in the finer vertical resolution experiment as compared to the standard vertical resolution. ~~Adding all natural and anthropogenic factors, as well as the contribution from finer vertical resolution, we estimate a total modeled warming of 1.7around the TTL (Table 3), which is higher than the observed 1.0warming from GPS-RO data.~~ However, in reality non-linear interactions between the different factors occur which we did not take into account in our first order linear approach. The comprehensive impact of all factors on the recent TTL warming can be estimated by the W_Aerosol run. The W_Aerosol run, with almost all observed forcings considered in this study, can be seen as the most realistic simulation. The TTL warming in the W_Aerosol run is ~~1.0~~0.9 K decade^{-1} on average and 1.6 K decade^{-1} in maximum (Fig. 7b), which are very close to the observed trend.

According to our experiments, one of the primary factors contributing to the recent warming in the TTL is the natural variability in tropical SSTs. However, the mechanism of the TTL response to SSTs awaits further investigation. One key issue is how much improvement

we can expect from using a fully-coupled ocean-atmosphere model instead of atmosphere only model with prescribed SSTs. Our W_L66 and W_L103 simulations indicate that the atmosphere-only model may not correctly reproduce the response of TTL variability to SST, but can be improved with finer vertical resolution.

Another important factor in contributing to the recent warming in the TTL is the QBO~~amplitude~~. The QBO ~~amplitude~~ is closely related to the tropical upwelling ~~.~~ Flury et al. (2013). A regression of temperature differences onto the differences in the vertical component of BDC between the Natural and NOQBO run, shows a very similar result than the regression of temperature differences onto the QBO time series (not shown). The QBO may influence the TTL temperature by modifying the BDC.

Fig. S3 clearly shows decadal to multidecadal fluctuations in TTL temperatures from both, the Modern Era Retrospective-analysis for Research and Applications (MERRA) reanalysis data, and our Natural and RCP85 runs, which provide strong support to the internal variability dominated TTL warming over the past decade.

The external forcings (solar, GHGs, ODS) contribute relatively little to the temperature variability in the TTL, except for the stratospheric aerosols. Internal variability, i.e. the QBO and tropical SSTs, seem to be mainly responsible for the recent TTL warming.

Acknowledgements. W. Wang is supported by a fellowship of the China Scholarship Council (CSC) at FU Berlin. This work was also performed within the Helmholtz-University Young Investigators Group NATHAN, funded by the Helmholtz-Association through the president's Initiative and Networking Fund, and the GEOMAR – Helmholtz-Zentrum für Ozeanforschung in Kiel. The model calculations have been performed at the Deutsche Klimarechenzentrum (DKRZ) in Hamburg, Germany. We thank F. Hansen, C. Petrick, R. Thiéblemont and S. Wahl for carrying out some of the simulations. We appreciate discussion about the statistical methods with D. Maraun and the help with grammar checking of L. Neef .

The service charges for this open access publication have been covered by a Research Centre of the Helmholtz Association.

References

Andrews, D. G.: An Introduction to Atmospheric Physics, Cambridge University Press, New York, 2010.

Andrews, D. G., Holton, J. R., and Leovy, C. B.: Middle Atmosphere Dynamics, vol. 40, Academic Press, San Diego, 1987.

Baldwin, M. P., Gray, L. J., Dunkerton, T. J., Hamilton, K., Haynes, P. H., Randel, W. J., Holton, J. R., Alexander, M. J., Hirota, I., Horinouchi, T., Jones, D. B. A., Kinnersley, J. S., Marquardt, C., Sato, K., and Takahashi, M.: The quasi-biennial oscillation, Rev. Geophys., 39, 179–229, doi:10.1029/1999RG000073, 2001.

Balmaseda, M. A., Trenberth, K. E., and Källén, E.: Distinctive climate signals in reanalysis of global ocean heat content, Geophys. Res. Lett., 40, 1754–1759, doi:10.1002/grl.50382, 2013.

Bourassa, A. E., Robock, A., Randel, W. J., Deshler, T., Rieger, L. A., Lloyd, N. D., Llewellyn, E. T., and Degenstein, D. A.: Large volcanic aerosol load in the stratosphere linked to Asian monsoon transport, Science, 337, 78–81, doi:10.1126/science.1219371, 2012.

Bunzel, F. and Schmidt, H.: The Brewer–Dobson circulation in a changing climate: impact of the model configuration, J. Atmos. Sci., 70, 1437–1455, doi:10.1175/JAS-D-12-0215.1, 2013.

Butchart, N.: The Brewer–Dobson circulation, Rev. Geophys., 52, 157–184, doi:10.1002/2013RG000448, 2014.

Butchart, N., Cionni, I., Eyring, V., Shepherd, T. G., Waugh, D. W., Akiyoshi, H., Austin, J., Bruhl, C., Chipperfield, M. P., Cordero, E., Dameris, M., Deckert, R., Dhomse, S., Frith, S. M., Garcia, R. R., Gettelman, A., Giorgetta, M. A., Kinnison, D. E., Li, F., Mancini, E., McLandress, C., Pawson, S., Pitari, G., Plummer, D. A., Rozanov, E., Sassi, F., Scinocca, J. F., Shibata, K., and Tian, W.: Chemistry-climate model simulations of twenty-first century stratospheric climate and circulation changes, J. Climate, 23, 5349–5374, doi:10.1175/2010JCLI3404.1, 2010.

Dessler, A. E., Schoeberl, M. R., Wang, T., Davis, S. M., and Rosenlof, K. H.: Stratospheric water vapor feedback., P. Natl. Acad. Sci. USA, 110, 18087–18091, doi:10.1073/pnas.1310344110, 2013.

Dessler, A., Schoeberl, M., Wang, T., Davis, S., Rosenlof, K., and Vernier, J.-P.: Variations of stratospheric water vapor over the past three decades, J. Geophys. Res., 119, 12–588, doi:10.1002/2014JD021712, 2014.

Engel, A., Mobius, T., Bonisch, H., Schmidt, U., Heinz, R., Levin, I., Atlas, E., Aoki, S., Nakazawa, T., Sugawara, S., Moore, F., Hurst, D., Elkins, J., Schauffler, S., Andrews, A., and Boering, K.: Age of stratospheric air unchanged within uncertainties over the past 30 years, Nat. Geosci., 2, 28–31, doi:10.1038/ngeo388, 2009.

England, M. H., McGregor, S., Spence, P., Meehl, G. A., Timmermann, A., Cai, W., Gupta, A. S., McPhaden, M. J., Purich, A., and Santoso, A.: Recent intensification of wind-driven circulation in the Pacific and the ongoing warming hiatus, Nature Climate Change, 4, 222–227, doi:10.1038/nclimate2106, 2014.

Flannaghan, T. and Fueglistaler, S.: The importance of the tropical tropopause layer for equatorial Kelvin wave propagation, J. Geophys. Res., 118, 5160–5175, doi:10.1002/jgrd.50418, 2013.

Flury, T., Wu, D. L., and Read, W. G.: Variability in the speed of the Brewer–Dobson circulation as observed by Aura/MLS, Atmos. Chem. Phys., 13, 4563–4575, doi:10.5194/acp-13-4563-2013, 2013.

Fueglistaler, S., Dessler, A., Dunkerton, T., Folkins, I., Fu, Q., and Mote, P. W.: Tropical tropopause layer, Rev. Geophys., 47, 1004, doi:10.1029/2008RG000267, 2009.

Fueglistaler, S., Liu, Y., Flannaghan, T., Haynes, P., Dee, D., Read, W., Remsberg, E., Thomason, L., Hurst, D., Lanzante, J., et al.: The relation between atmospheric humidity and temperature trends for stratospheric water, J. Geophys. Res., 118, 1052–1074, doi:10.1002/jgrd.50157, 2013.

Fyfe, J. C. and Gillett, N. P.: Recent observed and simulated warming, Nature Clim. Change, 4, 150–151, doi:10.1038/nclimate2111, 2014.

Fyfe, J. C., Gillett, N. P., and Zwiers, F. W.: Overestimated global warming over the past 20 years, Nature Climate Change, 3, 767–769, doi:10.1038/nclimate1972, 2013.

Gettelman, A. and Birner, T.: Insights into tropical tropopause layer processes using global models, J. Geophys. Res., 112, D23104, doi:10.1029/2007JD008945, 2007.

Gettelman, A. and Forster, P. D. F.: A climatology of the tropical tropopause layer, J. Meteor. Soc. Jpn., 80, 911–924, doi:10.2151/jmsj.80.911, 2002.

Gettelman, A., Birner, T., Eyring, V., Akiyoshi, H., Bekki, S., Brühl, C., Dameris, M., Kinnison, D. E., Lefevre, F., Lott, F., Mancini, E., Pitari, G., Plummer, D. A., Rozanov, E., Shibata, K., Stenke, A., Struthers, H., and Tian, W.: The Tropical Tropopause Layer 1960–2100, Atmos. Chem. Phys., 9, 1621–1637, doi:10.5194/acp-9-1621-2009, 2009.

Gray, L. J., Beer, J., Geller, M., Haigh, J. D., Lockwood, M., Matthes, K., Cubasch, U., Fleitmann, D., Harrison, G., Hood, L., Luterbacher, J., Meehl, G. A., Shindell, D., van Geel, B., and White, W.: Solar influences on climate, Rev. Geophys., 48, RG4001, doi:10.1029/2009RG000282, 2010.

Grise, K. M. and Thompson, D. W.: Equatorial planetary waves and their signature in atmospheric variability, J. Atmos. Sci., 69, 857–874, doi:10.1175/JAS-D-11-0123.1, 2012.

Grise, K. M. and Thompson, D. W.: On the signatures of equatorial and extratropical wave forcing in tropical tropopause layer temperatures, J. Atmos. Sci., 70, 1084–1102, doi:10.1175/JAS-D-12-0163.1, 2013.

Hansen, F., Matthes, K., and Gray, L.: Sensitivity of stratospheric dynamics and chemistry to QBO nudging width in the chemistry–climate model WACCM, J. Geophys. Res., 118, 10–464, doi:10.1002/jgrd.50812, 2013.

Kawatani, Y. and Hamilton, K.: Weakened stratospheric quasibiennial oscillation driven by increased tropical mean upwelling, Nature, 497, 478–481, doi:10.1038/nature12140, 2013.

Kim, J., Grise, K. M., and Son, S.: Thermal characteristics of the cold-point tropopause region in CMIP5 models, J. Geophys. Res., 118, 8827–8841, doi:10.1002/jgrd.50649, 2013.

Kosaka, Y. and Xie, S.-P.: Recent global-warming hiatus tied to equatorial Pacific surface cooling, Nature, 501, 403–407, doi:10.1038/nature12534, 2013.

Lean, J., Rottman, G., Harder, J., and Kopp, G.: SORCE contributions to new understanding of global change and solar variability, Sol. Phys., 230, 27–53, doi:10.1007/s11207-005-1527-2, 2005.

Li, F., Austin, J., and Wilson, J.: The strength of the Brewer–Dobson circulation in a changing climate: coupled chemistry-climate model simulations, J. Climate, 21, 40–57, doi:10.1175/2007JCLI1663.1, 2008.

Lin, P. and Fu, Q.: Changes in various branches of the Brewer–Dobson circulation from an ensemble of chemistry climate models, J. Geophys. Res., 118, 73–84, doi:10.1029/2012JD018813, 2013.

Marsh, D. R., Mills, M. J., Kinnison, D. E., Lamarque, J.-F., Calvo, N., and Polvani, L. M.: Climate change from 1850 to 2005 simulated in CESM1 (WACCM), J. Climate, 26, 7372–7391, doi:10.1175/JCLI-D-12-00558.1, 2013.

Matthes, K., Marsh, D. R., Garcia, R. R., Kinnison, D. E., Sassi, F., and Walters, S.: Role of the QBO in modulating the influence of the 11 year solar cycle on the atmosphere using constant forcings, J. Geophys. Res., 115, 18110, doi:10.1029/2009JD013020, 2010.

Meehl, G. A., Washington, W. M., Arblaster, J. M., Hu, A., Teng, H., Tebaldi, C., Sanderson, B. N., Lamarque, J.-F., Conley, A., Strand, W. G., and White, J. B.: Climate system response

to external forcings and climate change projections in CCSM4, J. Climate, 25, 3661–3683, doi:10.1175/JCLI-D-11-00240.1, 2012.

Meinshausen, M., Smith, S. J., Calvin, K., Daniel, J. S., Kainuma, M. L. T., Lamarque, J.-F., Matsumoto, K., Montzka, S., Raper, S., Riahi, K., Thomson, A., Velders, G. J. M., and van Vuuren, D. P.: The RCP greenhouse gas concentrations and their extensions from 1765 to 2300, Climatic Change, 109, 213–241, doi:10.1007/s10584-011-0156-z, 2011.

Morgenstern, O., Giorgetta, M. A., Shibata, K., Eyring, V., Waugh, D. W., Shepherd, T. G., Akiyoshi, H., Austin, J., Baumgaertner, A. J. G., Bekki, S., Braesicke, P., Brühl, C., Chipperfield, M. P., Cugnet, D., Dameris, M., Dhomse, S., Frith, S. M., Garny, H., Gettelman, A., Hardiman, S. C., Hegglin, M. I., Jöckel, P., Kinnison, D. E., Lamarque, J.-F., Mancini, E., Manzini, E., Marchand, M., Michou, M., Nakamura, T., Nielsen, J. E., Olivié, D., Pitari, G., Plummer, D. A., Rozanov, E., Scinocca, J. F., Smale, D., Teyssèdre, H., Toohey, M., Tian, W., and Yamashita, Y.: Review of the formulation of present-generation stratospheric chemistry-climate models and associated external forcings, J. Geophys. Res., 115, D00M02, doi:10.1029/2009JD013728, 2010.

Neely, R. R., Toon, O. B., Solomon, S., Vernier, J. P., Alvarez, C., English, J. M., Rosenlof, K. H., Mills, M. J., Bardeen, C. G., Daniel, J. S., and Thayer, J. P.: Recent anthropogenic increases in SO_2 from Asia have minimal impact on stratospheric aerosol, Geophys. Res. Lett., 40, 999–1004, doi:10.1002/grl.50263, 2013.

Oberländer, S., Langematz, U., and Meul, S.: Unraveling impact factors for future changes in the Brewer–Dobson circulation, J. Geophys. Res., 118, 10–296, doi:10.1002/jgrd.50775, 2013.

Randel, W. J. and Jensen, E. J.: Physical processes in the tropical tropopause layer and their roles in a changing climate, Nat. Geosci., 6, 169–176, doi:10.1038/ngeo1733, 2013.

Randel, W. J., Shine, K. P., Austin, J., Barnett, J., Claud, C., Gillett, N. P., Keckhut, P., Langematz, U., Lin, R., Long, C., Mears, C., Miller, A., Nash, J., Seidel, D. J., Thompson, D. W. J., Wu, F., and Yoden, S.: An update of observed stratospheric temperature trends, J. Geophys. Res., 114, D02107, doi:10.1029/2008JD010421, 2009.

Richter, J. H., Solomon, A., and Bacmeister, J. T.: On the simulation of the quasi-biennial oscillation in the Community Atmosphere Model, version 5, Journal of Geophysical Research: Atmospheres, 119, doi:10.1002/2013JD021122, 2014.

Schmidt, T., Wickert, J., and Haser, A.: Variability of the upper troposphere and lower stratosphere observed with GPS radio occultation bending angles and temperatures, Adv. Space. Res., 46, 150–161, doi:10.1016/j.asr.2010.01.021, 2010.

Shepherd, T. G. and McLandress, C.: A robust mechanism for strengthening of the Brewer–Dobson circulation in response to climate change: critical-layer control of subtropical wave breaking, J. Atmos. Sci., 68, 784–797, doi:10.1175/2010JAS3608.1, 2011.

Simpson, I. R., Blackburn, M., and Haigh, J. D.: The role of eddies in driving the tropospheric response to stratospheric heating perturbations, J. Atmos. Sci., 66, 1347–1365, doi:10.1175/2008JAS2758.1, 2009.

Solomon, S., Rosenlof, K. H., Portmann, R. W., Daniel, J. S., Davis, S. M., Sanford, T. J., and Plattner, G.-K.: Contributions of stratospheric water vapor to decadal changes in the rate of global warming, Science, 327, 1219–1223, doi:10.1126/science.1182488, 2010.

Solomon, S., Daniel, J., Neely, R., Vernier, J.-P., Dutton, E., and Thomason, L.: The persistently variable "background" stratospheric aerosol layer and global climate change, Science, 333, 866–870, doi:10.1126/science.1206027, 2011.

SPARC-CCMVal: SPARC Report on the Evaluation of Chemistry-Climate Models, SPARC Report 5, WCRP-132, WMO/TD-1526, 2010.

Stiller, G. P., von Clarmann, T., Haenel, F., Funke, B., Glatthor, N., Grabowski, U., Kellmann, S., Kiefer, M., Linden, A., Lossow, S., and López-Puertas, M.: Observed temporal evolution of global mean age of stratospheric air for the 2002 to 2010 period, Atmos. Chem. Phys., 12, 3311–3331, doi:10.5194/acp-12-3311-2012, 2012.

Wang, J. S., Seidel, D. J., and Free, M.: How well do we know recent climate trends at the tropical tropopause?, J. Geophys. Res., 117, 09 118, doi:10.1029/2012JD017444, 2012.

Wang, W., Matthes, K., Schmidt, T., and Neef, L.: Recent variability of the tropical tropopause inversion layer, Geophys. Res. Lett., 40, 6308–6313, doi:10.1002/2013GL058350, 2013.

Wigley, T.: Appendix A: Statistical issues regarding trends, in: Temperature Trends in the Lower Atmosphere: Steps for Understanding and Reconciling Differences, edited by: Karl, T. R., Hassol, S. J., Miller, C. D., and Murray, W. L., A Report by Climate Change Science Program and the Subcommittee on Global Change Research, Washington, DC, USA, UNT Digital Library, 129–139, 2006.

Zhou, X.-L., Geller, M. A., and Zhang, M.: Cooling trend of the tropical cold point tropopause temperatures and its implications, J. Geophys. Res., 106, 1511–1522, doi:10.1029/2000JD900472, 2001.

Table 1. Overview of fully-coupled CESM-WACCM simulations (1955–2099).

Simulations	Natural Forcings	GHGs
Natural	All natural forcings, including transit solar variability, fully coupled ocean, prescribed volcanic aerosols and nudged QBO	Fixed GHGs to 1960s state
SolarMean	As Natural run, but with fixed solar radiation	Fixed
FixedSST	As Natural run, but with fixed SSTs	Fixed
NOQBO	As Natural run, but without QBO nudging	Fixed
RCP85	As Natural run	RCP8.5 scenario

Table 2. Overview of WACCM atmospheric stand-alone simulations (2001–2010).

Simulations	Number of Simulations	Vertical levels	Forcings	Stratospheric aerosols
W_L103	3	103	Observed solar variability and SSTs, nudged QBO, GHGs in RCP4.5 scenario	Volcanic aerosols from CCMVal-2
W_L66	3	66	As W_L103	As W_L103
W_Aerosol	1	103	As W_L103	Stratospheric aerosols from CCMI

Table 3. Summary of contributions from the varying factors to the observed TTL warming between 2001 and 2011, in the region 20° S–20° N latitude and 16–20 km.

Factors	Solar	SSTs	QBO	GHGs	Aerosols	~~Vertical Resolution~~ **Total**
Contribution (K decade^{-1})	~~0.3~~ 0.2	~~0.4~~ 0.3	~~0.5~~ 0.2	~~0.1~~ 0.0	~~0.4~~ 0.2	~~0.8~~ ~~1.7~~**0.5**
Observation						**0.9**
Vertical Resolution	~~1.0~~					0.8

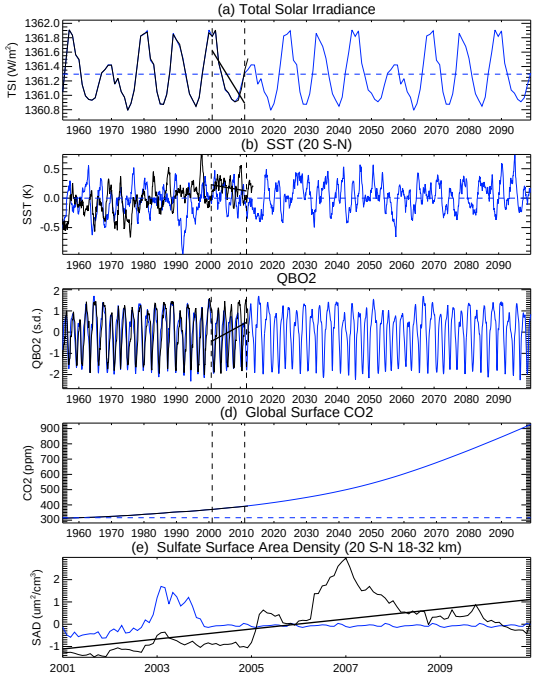
(a) Total Solar Irradiance
TSI (W/m²)
1362.0
1361.8
1361.6
1361.4
1361.2
1361.0
1360.8
1960 1970 1980 1990 2000 2010 2020 2030 2040 2050 2060 2070 2080 2090
(b) SST (20 S-N)
SST (K)
0.5
0.0
-0.5
1960 1970 1980 1990 2000 2010 2020 2030 2040 2050 2060 2070 2080 2090
QBO2
QBO2 (s.d.)
2
1
0
-1
-2
1960 1970 1980 1990 2000 2010 2020 2030 2040 2050 2060 2070 2080 2090
(d) Global Surface CO2
CO2 (ppm)
900
800
700
600
500
400
300
1960 1970 1980 1990 2000 2010 2020 2030 2040 2050 2060 2070 2080 2090
(e) Sulfate Surface Area Density (20 S-N 18-32 km)
SAD (um²/cm³)
2
1
0
-1
2001 2003 2005 2007 2009

Figure 1. Time series of forcing data sets used for the simulations from 1955 through 2099. **(a)** TSI from observations (black)until 2012, the *Natural* run (solid blue) and the *SolarMean* run (dashed blue) runs. The last four solar cycles have been repeated into the future. **(b)** SSTs SST anomalies from observations HadISSTs (see details in text) (black), the *Natural* run (solid blue) and the *FixedSST* run (dashed blue) runs. The SSTs in **(c)** QBO2 (see text for details) from observations (black) and the *Natural* run have been smoothed by a low-pass ($T > 30$yearssolid blue) Butterworth Filterrun. The smooth blue line has been smoothed twice by the same low-pass Butterworth Filter. **(c)** Same as in **(b)**, but for the QBO amplitude calculated from zonal mean zonal winds at 70and between 10S and 10N. **(d)** Global surface CO_2 concentration from observations (black, overlapped with the blue line), the *RCP85* run (solid blue) and the *Natural* run (dashed blue) runs. **(e)** AOD (532 nm, 18–32 km) from the CCMI (Solid blueblack) and the CCMVal2 (blackblue) projects for the time 2001–2010. The blue black solid straight lines in each subfigure are the linear fits of the respective forcing for the selected decadeduring 2001-2011.

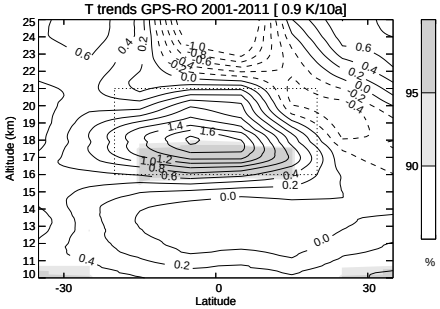

Figure 2. Latitude-height section of linear temperature trends over the past decade (2001–2011) from *GPS-RO* data over a height range from 10 to 25 km and 35° S to 35° N latitude; contour interval: 0.2 K decade^{-1}. Grey shading represents the statistical significance for the trends. ~~See text for details on the linear trend and the statistical significance calculation.~~

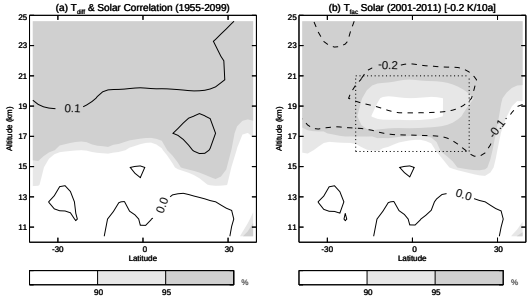

Figure 3. ~~**(a, b)**~~ **(a)** Latitude-height sections of ~~composite~~ correlations between temperature ~~trends over selected time periods~~ differences (~~1958–1968, 2001–2011, 2045–2055, and 2089–2099, see Fig. 1~~*Natural* - *SolarMean*) ~~from~~ and solar TSI in the *Natural* ~~and *SolarMean* runs, respectively~~run over the whole period (1955-2099); contour interval: ~~0.2~~0.1; Grey shading represents statistically significant correlations, with Students' T test. ~~**(c)** The differences between **(a)** and~~ **(b)** The regressed contributions of solar TSI to the TTL temperature trends during 2001-2011 (Eq. 2); contour interval: 0.1 K decade^{-1}; Grey shading represents statistically significant ~~trends~~regressions. See text for details on the calculation of the ~~composite~~ regressed trend, and the testing of the statistical significance. The decadal temperature trend in the title is the mean value from the dashed box.

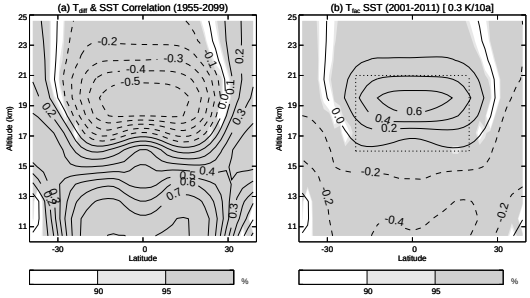

Figure 4. ~~**(a, b)** Latitude-height sections of composite temperature trends over selected time periods (1956–1968, 1980–1991, 2001–2014, 2028–2043, 2047–2057, see~~ Same as Fig. ~~1~~3) ~~from~~ , but for the impact of tropical SSTs by comparing the *Natural* and *FixedSST* runs~~, respectively;~~ . contour interval: **(a)** 0.1 and **(b)** 0.2 K decade^{-1}.~~**(c)** The differences between **(a)** and **(b)**. Grey shading as in Fig. 3.~~

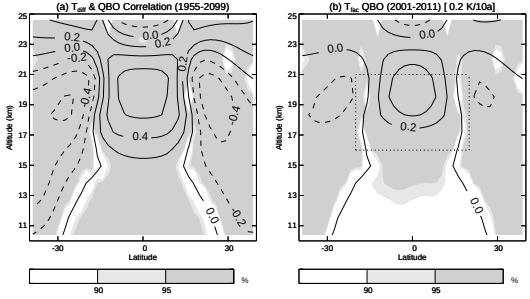

Figure 5. Same as Fig. 3, but for the impact of the ~~QBO amplitude on temperature trends **(c)**~~ QBO2 (see text for details) by comparing the *Natural* and the *NOQBO* experiments~~**(a, b)** for the periods 2003–2017 and 2054–2068 (see Fig. 1)~~; contour interval: **(a)** 0.2 and **(b)** 0.2 K decade^{-1}.

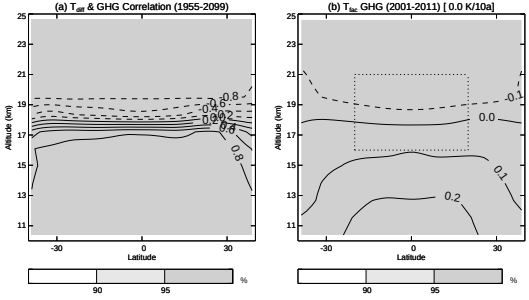

Figure 6. Same as Fig. 3, but for the impact of anthropogenic forcings (GHGs~~and ODS~~) ~~on temperature trends~~ by comparing the *Natural* and ~~*RCP85*~~ *RCP85* experiments~~**(a, b) for the period 2001–2050**~~; contour interval: **(a)** 0.2 and **(b)** 0.1 K decade^{-1}.

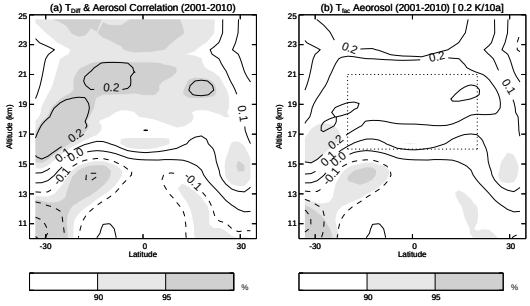

Figure 7. Same as Fig. 3, but for the impact of stratospheric aerosols ~~on temperature trends~~ by comparing the *W_L103* and the *W_Aerosol* ~~experiment **(a, b)** for the period 2001–2010;~~ experiments. contour interval: ~~0.2~~**(a)** 0.1 and **(b)** 0.1 K decade^{-1}. The ~~temperature trends~~ temperatures in the *W_L103* run were calculated ~~by~~ from a three member ensemble mean.

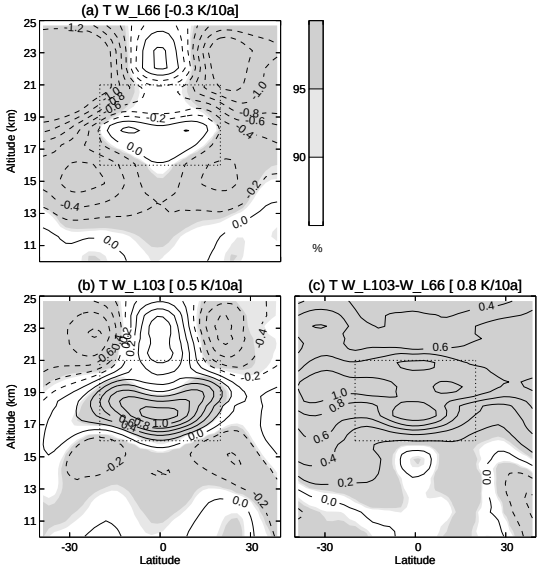

Figure 8. ~~Same as Fig. 3, but for the impact~~ **(a, b)** Latitude-height sections of ~~the differences in vertical resolution on~~ temperature trends **(c)** ~~by comparing~~ over 2001-2010 from the *W_L103* and *W_L66* experiments**(a, b)** ~~for the period 2001–2010;~~ , respectively. **(c)** The differences between **(a)** and **(b)**. contour interval: 0.2 K decade^{-1} and grey shading ~~as in Fig~~represents statistically significant trends. ~~3.~~ The temperature trends in the *W_L103* and *W_L66* runs are calculated by multiple linear regression for ~~the~~ each three ~~ensembles~~simulations.

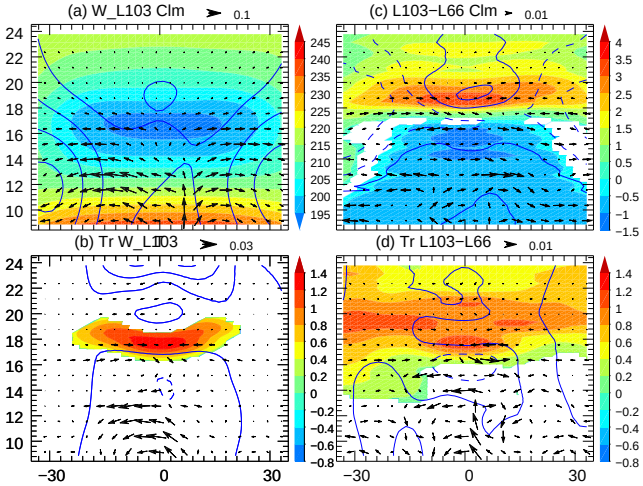

Figure 9. (a) Annual mean climatological zonal mean zonal wind (contours, contour interval 10 m s^{-1}, dashed lines indicate easterly winds), BDC vector (arrows, scaled with the square root of pressure) and temperature (colour shadings) for the *W_L103* experiment from 8 to 25 km and 35° S through 35° N. **(c)** Differences of the zonal mean zonal wind (contour interval 1.0 m s^{-1}), BDC vector and temperature (colour shadings indicate 95 % statistical significances) between the *W_L103* and the *W_L66* experiments. (**b** and **d**) Same as **(a)** and **(c)**, but for the linear trends from 2001 to 2010. The shadings in **(b)** and **(d)** indicate 95 % statistical significance. The contour intervals are 2 m s^{-1} and 1 m s^{-1} in **(c)** and **(d)**, respectively.